EURASIP Journal on Advances in Signal Processing
a SpringerOpen Journal

REVIEW ARTICLE Open Access

An overview of GNSS remote sensing

Kegen Yu[1*], Chris Rizos[2], Derek Burrage[3], Andrew G Dempster[4], Kefei Zhang[5] and Markus Markgraf[6]

Abstract

The Global Navigation Satellite System (GNSS) signals are always available, globally, and the signal structures are well known, except for those dedicated to military use. They also have some distinctive characteristics, including the use of L-band frequencies, which are particularly suited for remote sensing purposes. The idea of using GNSS signals for remote sensing - the atmosphere, oceans or Earth surface - was first proposed more than two decades ago. Since then, GNSS remote sensing has been intensively investigated in terms of proof of concept studies, signal processing methodologies, theory and algorithm development, and various satellite-borne, airborne and ground-based experiments. It has been demonstrated that GNSS remote sensing can be used as an alternative passive remote sensing technology. Space agencies such as NASA, NOAA, EUMETSAT and ESA have already funded, or will fund in the future, a number of projects/missions which focus on a variety of GNSS remote sensing applications. It is envisaged that GNSS remote sensing can be either exploited to perform remote sensing tasks on an independent basis or combined with other techniques to address more complex applications. This paper provides an overview of the state of the art of this relatively new and, in some respects, underutilised remote sensing technique. Also addressed are relevant challenging issues associated with GNSS remote sensing services and the performance enhancement of GNSS remote sensing to accurately and reliably retrieve a range of geophysical parameters.

Review

Recent developments in both ground-based and satellite-borne geospatial infrastructure have opened exciting new opportunities for geodesists to contribute to 'big issues' such as weather, climate, global warming, environment and sustainability. The ability to remotely sense the atmosphere using geodetic techniques has dramatically improved over the past decade, primarily as a result of advances in satellite-borne technologies, large-scale and dense geodetic Global Navigation Satellite System (GNSS) networks, new dedicated space missions and developments of new algorithms and innovative methodologies. Atmospheric sounding is a new area of GNSS applications based on the analysis of radio signals from GNSS satellites, which are refracted as they pass through the atmosphere and can give information on its physical properties. Depending on the way the signals (direct or reflected) are used, GNSS remote sensing can be broadly divided into two categories: GNSS reflectometry (GNSS-R) and GNSS refractometry (known as GNSS radio occultation or GNSS-RO). GNSS-R involves analysing measurements of GNSS signals reflected from the Earth's surface, while GNSS-RO utilises measurements of GNSS signals refracted by the atmosphere when the slanted propagation path is close to the Earth's limb. In the following sections more details about the theory and practice of GNSS remote sensing are provided. Interested readers are also referred to [1,2] for more background information.

Atmospheric sensing via GNSS meteorology

The use of GNSS receivers installed on low Earth orbit (LEO) satellites to measure the refracted radio signals (GNSS-RO) coupled with ground-based atmospheric sounding techniques that use continuously operating reference station (CORS) networks for the determination of water vapour (WV) variability form the basis for GNSS meteorology. The dynamics of WV have a strong influence on weather and climate due to the large energy transfers in the hydrological processes. This is particularly so during the formation and life cycle of severe mesoscale convective storm and precipitation systems. Contrary to its importance, WV remains poorly understood and inadequately measured both spatially and temporally, especially in the southern hemisphere, where meteorological data are sparse.

* Correspondence: kgyu@sgg.whu.edu.cn
[1]School of Geodesy and Geomatics, Wuhan University, Wuhan 430079, China
Full list of author information is available at the end of the article

GNSS atmospheric remote sensing using LEO satellites such as CHAllenging Minisatellite Payload (CHAMP), Gravity Recovery and Climate Experiment (GRACE) and Constellation Observing System for Meteorology, Ionosphere, and Climate (COSMIC) is a robust technique for profiling the atmosphere from LEO satellite orbit heights down to the Earth's surface [3-5]. Many studies have demonstrated that the GNSS-RO technique is able to measure the Earth's atmospheric parameters with unprecedented high accuracy, high resolution and global coverage [6-10]. RO has been considered as a new observation type for meteorology which has the capability to provide significant information on the thermodynamic state of the atmosphere and to allow improvements in atmospheric analysis and prognosis. GPS RO has been operationally used in numerical weather prediction (NWP) models for weather forecasting by major weather forecasting centres such as those in the USA, Europe and Australia, since 2006. The beneficial impact of such data assimilation has been quantified in several studies [11-14], and it is significant particularly in data-void regions (e.g. southern hemisphere). GNSS-RO has been shown to significantly reduce both the forecast errors in the ECMWF system and NWP model biases. It has become the independent sensor technique with the fifth highest impact in operational weather forecasting, among the 24 available systems [12-15]. Most recently, Le Marshall et al. [11] have successfully assimilated MetOp, GRACE and COSMIC RO data into the Australian weather forecasting model (ACCESS) using 4DVAR, and a reliability improvement of 10 h has been achieved in a 1- to 5-day period. GPS RO has been officially used in operational Australian ACCESS system since late 2011.

Building on the success of the COSMIC RO mission, a follow-on mission (COSMIC-2) was recently approved by the USA and Taiwan that will launch six satellites into low-inclination orbits in late 2015 and another six satellites into high-inclination orbits in early 2018. Up to 12,000 high-quality profiles per day will be tracked when it is fully deployed. This revolutionary increase in the number of atmospheric and ionospheric observations will greatly benefit the research and operational communities and will open up unprecedented research opportunities for hurricane analysis and prediction, and studies of Madden-Julian Oscillation and climate processes, to name just a few. In addition, algorithm development, optimisation and refinement, error reduction, climate analysis and benchmarking, and polar applications are all frontier areas of RO research [15-21].

Vertical gradients of the atmospheric properties are retrieved from precise measurements of the radio propagation path between a LEO-based GPS receiver and an occulting GPS satellite transmitter pair. A radio occultation event (ROE) occurs when a GPS satellite is setting or rising behind the Earth's limb as viewed by a receiver onboard a LEO satellite as shown in Figure 1. During a ROE, the transmitted signals from the GPS to the LEO satellite are delayed. This delay can be converted into a profile of bending angles and consequently processed to produce a refractivity index profile. The refractivity is a function of the electron density in the ionosphere, and temperature, pressure and WV in the atmosphere. The fundamental GPS observation equation based upon which atmospheric parameters are retrieved can be expressed as follows:

$$L = \rho + c(\delta t_{\mathrm{clk}} - \delta t_{\mathrm{rel}}) - c(\delta T_{\mathrm{clk}} - \delta T_{\mathrm{rel}}) + N \cdot \lambda + \Delta\varphi_{\mathrm{excess}} + \Delta R + \varepsilon \quad (1)$$

where L is the raw GPS carrier phase measurement, ρ is the geometric distance between the LEO and GPS satellites, c is the speed of light, (δt_{clk}, δt_{rel}) are the errors related to the clock and relativistic effects of LEO, (δT_{clk}, δT_{rel}) are the errors related to GPS satellite clock and relativistic effects, N is the integer ambiguity, λ is the wavelength of the GPS L-band signal, $\Delta\varphi_{\mathrm{excess}}$ is the excess phase along the radio signal propagation path which is the phase increment due to the signal propagation delay, ΔR is the general relativistic effect, and ε is the measurement noise. Figure 2 shows the flowchart of a typical GNSS-RO atmospheric retrieval process, and Figure 3 shows a typical 1-day RO event distribution across the globe under a full COSMIC constellation.

The L-band radio signals broadcast by the GNSS satellites are affected by both the ionospheric and tropospheric effects as they travel through the atmosphere to the permanent ground-based GNSS receivers. Using a dense CORS network, the impact of the neutral atmosphere, i.e. tropospheric delays, can be estimated as a by-product of the geodetic data processing. This ground-based GNSS meteorology is currently used to produce two different data products. Firstly, the integrated precipitable WV in the zenith direction above each GPS station can be accurately estimated using path delay measurements between a receiver and GPS satellites. Secondly, the spatial and temporal distribution of wet refractivity can be reconstructed using accurate measurements of path delays between each satellite-and-receiver link over the GNSS network. This method is called GNSS tomography which is an emerging method for 4D tropospheric reconstruction using a local GNSS CORS network. Integrated measurements of wet delays are extracted from each satellite-to-station link, which are used as the primary observable through a finite 3D grid field to estimate the time-dependent 3D structure of WV. An integrated approach is usually used in the tomographic reconstruction process by incorporating multiple sources of measurements from GNSS CORS,

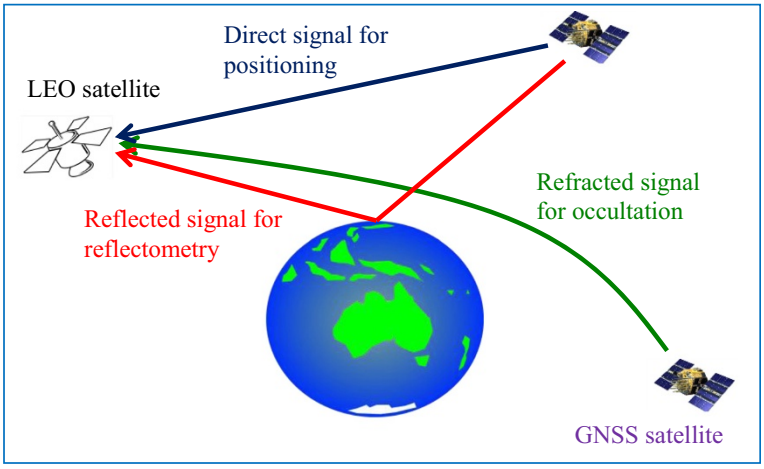

Figure 1 Illustration of the geometry of the direct, reflected and refracted GNSS signals and their use for different applications.

automated weather stations, radiosonde, RO and NWP models.

A variety of research has been conducted based on both real and simulated data. For example, [22] presented a simulation and real data investigation into 4D tropospheric tomography using GPS observations and a stochastic approach. The real data analysis used the Kilauea network in Hawaii with the voxel grid discretisation covering an area of 400 km^2 and 15 km in height. A Kalman filtering technique was used for estimating the evolution of dynamically changing parameters. An alternate method presented in [23] used raw GPS phase measurements directly for the reconstruction of WV distribution. This method was tested using simulations where the horizontal and vertical voxel resolution, observation noise and additional GNSS constellations were varied and optimised. Results indicated that high accuracy can be achieved in the modelling of wet refractivity in lower layers. However, its limitation was in resolving layers above 4,000 m altitude. Nilsson and Gradinarsky [24] investigated the benefits of GPS tomography for modelling mesoscale precipitation systems. The model was designed on the premise that the grid system would move in relation to the vector of horizontal wind velocity. It was concluded that GPS tomographic solutions can improve the initial WV field for short-term NWP predictions and forecasting. Bender and Raabe [25] extensively analysed the preconditions and constraints of ground-based GPS WV tomography and suggested that the spatial resolution is limited by the density of the ground-based GPS networks and the number of available GNSS satellites. To optimise horizontal resolution, the horizontal size of the humidity field voxels would be restricted to the mean interstation distance of the GPS network. Another important parameter presented is the elevation cutoff angle; the number of available rays increases heavily with a decreasing elevation cutoff angle and in return provides much more information on the lower troposphere. Rohm and colleagues [26,27] presented investigations into the concept of near-real-time atmospheric model construction based on the GNSS and meteorological observations. This nowcasting approach provides accurate comparisons with NWP analysis models. Yuan et al. [28] recently investigated real-time retrieval using precise point positioning technique and good results were obtained. Choy et al. [29] investigated the propagation and distribution of WV during the Melbourne severe weather event in 2010, while Manning and colleagues [30,31] investigated 4D

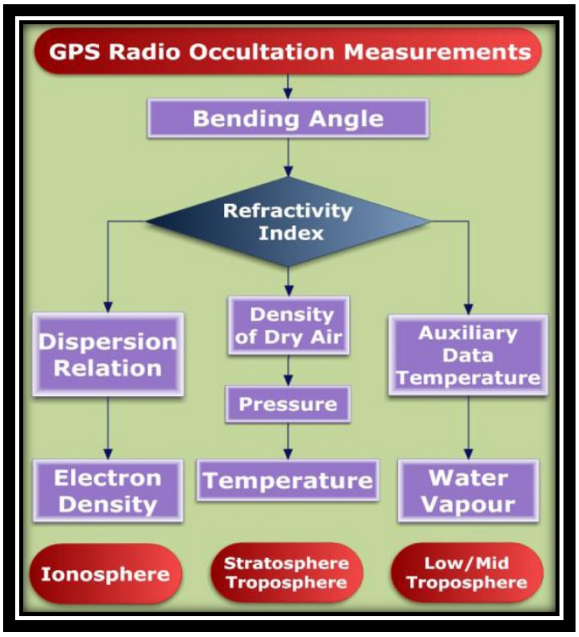

Figure 2 Typical data processing steps involved in GNSS-RO atmospheric retrievals.

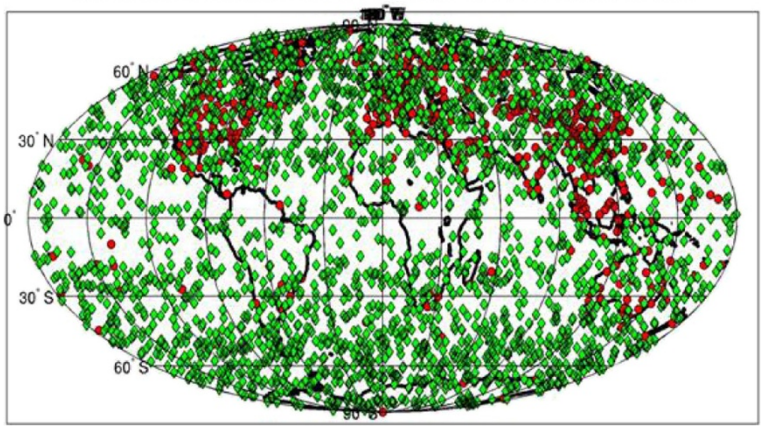

Figure 3 One-day RO event distribution across the globe under a full COSMIC constellation. GPS RO sounding locations for COSMIC (in green) and radiosonde sites (in red) in a period of 24 h (after UCAR).

methods of reconstructing wet refractivity fields using GPS tomography for the Australian region. A comprehensive investigation was carried out in terms of sensitivity analysis of multiple measurements, voxel optimisation, parameterisation method and Kalman filtering using two severe storm events in Melbourne as case studies. Bennitt and Jupp [32] studied the data assimilation of GPS zenith total delays into the Met Office NWP models, and a slight positive overall impact and significant improvements to short-range forecasts in some cases were demonstrated.

To summarise, GNSS is now an established atmospheric observing system which can accurately sense WV, the most abundant greenhouse gas, accounting for 60 to 70% of atmospheric warming. Severe weather forecasting is challenging, in part due to the high temporal and spatial variation of atmospheric WV. WV content is undersampled in the current meteorological and climate observing systems; obtaining and exploiting more high-quality humidity observations is essential to NWP data assimilation, nowcasting and climate monitoring. It is expected that the GNSS meteorology technology will significantly advance our knowledge of Earth's atmospheric structure and processes, including severe weather phenomena and climate change, in particular in data-sparse areas such as the southern hemisphere, and oceanic and polar regions.

Ocean observation

The complex temporal and spatial variations which shape the ocean surface are amenable to study using remote sensing methods because the sea surface both emits and strongly reflects electromagnetic radiation. Static ocean surface undulations are dominated by Earth's geoid and by its topographic response to the mean ocean circulation, while temporal departures from this surface are forced by weather and climate-related changes in ocean temperature and salinity, and surface wind stress. Lunar and solar gravitational tides, and their harmonics, contribute additional variability, on daily and longer timescales. These sea level changes, which also drive ocean currents, have been sensed remotely using nadir-viewing satellite-borne radar altimeters, almost continuously over the last four decades. Observations from these altimeters provide vital information for studies of deep-ocean circulation and boundary currents, the mid-ocean gyres, tsunamis and ocean currents on synoptic to global scales, while mesoscale (approximately 100 km) ocean eddies are only marginally resolved.

Finer-scale topographic changes associated with ocean surface roughness, or 'sea state', are dominated by locally forced wind-waves and swell from distant storms occurring on time and space scales exceeding a few hours and kilometres. In addition to their effects on shipping and other human activities, these contribute to ocean mixing, which crucially affects the exchange of momentum, heat, salt and various gases, such as CO_2, across the air-sea interface, with important implications for weather and climate studies. Sea state also affects the interaction of electromagnetic radiation with the sea surface through its impact on the effective emissivity and reflectivity of the surface. By using suitable remote sensing methods, its effects can be used to deduce sea state or mean square slope. Coupled with a wind-wave spectral model, the surface wind field can also be inferred. Alternatively, these effects can be used to derive corrections for roughness influence on retrievals of other geophysical parameters from microwave radiometers, such as sea surface salinity. Since sea state modifies the waveform of the radar reflection, nadir-viewing (monostatic) radar altimeters are also used to estimate wave height and wind speed, with high spatial resolution (approximately 7 km) along-track but poorer resolution (approximately 300 km) across-track

and with an approximately 10-day repeat cycle [33]. However, over the last three decades, a new approach to measuring sea surface height, wind speed and sea state bistatic radar, offering higher spatial and temporal resolution, and utilising GNSS satellites as transmitters has been proposed and developed.

Ocean observation using GNSS signals was first proposed as the Passive Reflectometry and Interferometry System (PARIS) concept to perform mesoscale ocean altimetry [34], and an in-orbit demonstrator has been designed to implement this concept [35]. Recent developments in GNSS-R altimetry include experimental ground-based and airborne campaigns, performance studies, refinements in error budget estimates and alternative signal processing methods for retrieving sea surface height estimates from GNSS-R instrumentation. The new methods exploit a variety of techniques for enhancing performance characterised by improvements to spatial and temporal resolutions, signal to noise ratio and/or accuracy and precision. With respect to error characterisation, Martin-Neira et al. [36] studied the effects of errors in delay drift compensation on the waveform and its impact on the altimetric accuracy and precision, while Pascual et al. [37] used simulated GPS and Galileo signals to investigate the impact of bandwidth and low-power transmitters on height accuracy and precision. Rius et al. [38] investigated the scatterometric and specular delay observables and considered various sources of uncertainty including observation statistics and model parameterisation or calibration error. Methodology studies include an investigation of model-free retrieval of sea surface height using a power ratio method combined with cost function optimisation when the sea surface is rather rough [39]. A semi-codeless processing approach [40] showed how to determine the phase sign variation of encrypted P-code GNSS signals and combine it with the CA signal stream to enhance signal to noise ratio in comparison with that achieved by the interferometric method. An investigation of Doppler multilook processing [41] realised enhanced spatial and temporal resolution by intra- and inter-Doppler tracking and averaging of delay waveforms. The method demonstrated 25 to 30% improvement in altimetric precision over the interferometric method and increased flexibility in trading off spatial resolution and height estimation accuracy. In a ground-based study reported in 2001 [33], retrieval of Crater Lake surface height to 2-cm precision was achieved using GPS altimetry from relatively low satellite elevations. A year later, 5-cm precision GPS ocean altimetry was achieved from an aircraft [42]. A ground-based experiment implementing the PARIS concept in the form of an X-band instrument [43] takes advantage of high signal to noise ratio (SNR) associated with X-band signals of opportunity from digital satellite TV broadcasts. Useful overviews including summaries of these and/or other GNSS altimetry studies appear in [2,44,45], along with an assessment of the overall performance of GNSS-R altimetry techniques.

Using airborne data collected in 1997, Garrison et al. [46] first demonstrated the potential for retrieving sea state from the dependence of the GNSS sea surface reflection waveform width on wind speed. This waveform represented the cross-correlation between a replica of the direct signal and the signal reflected off the sea surface, as a function of delay. Coupled with knowledge of the GPS navigation code autocorrelation function (which is usually triangular in shape), this gives an estimate of the radar cross section that is closely related to the ocean surface mean square slope and hence surface roughness. During the period 2003 to 2011, the UK-Disaster Monitoring Constellation (UK-DMC) satellite carried an experimental GNSS reflectometer, which yielded sea state and wind speed estimates for representative cases of low to moderate wind strength [47]. While suitable for scatterometric measurements, this instrument was not optimised for altimetric measurements.

Since Garrison's first experiment, a variety of techniques have been developed for retrieving surface mean square slope and wind speed, and many have been tested using ground and airborne field campaigns. The following discussion of some key studies exemplifies the progress made but is not meant to be comprehensive: Retrieval of ocean wind speeds from a balloon in the stratosphere [48] produced mean square slope and corresponding wind speed estimates departing from radiosondes and satellite altimeters and a scatterometer by at most 1 m/s in relatively calm winds (less than about 9 m/s). Retrieval of hurricane winds using GPS reflectometry was first demonstrated by Katzberg et al. [49] who later calibrated retrieved hurricane winds using dropsondes [50,51]. The GNSS-R reflectometer was found to underestimate observed winds, but a standard deviation around a linear regression fit to observations of about 5 m/s was found, for winds ranging from 10 to 40 m/s. Recently, wind speeds have been retrieved using GNSS-R instrumentation from an aircraft using scattering model-free linear regression of several Delay Doppler Map (DDM) observables [52]. The results obtained using satellite triplets, and validated using coincident dropsonde measurements, produced errors of up to 1 to 4 m/s for winds of 5 to 25 m/s, with overall accuracy and precision of the order of 1 to 2 m/s.

Methods to extract directional roughness characteristics have been developed and tested using airborne campaign data [53-55]. Wind direction retrieval is performed by accounting for differences in upwind/crosswind surface slope probability distribution, which is represented by an observable asymmetry in the glistening zone. The particular technique devised by Cardellach and Rius [55] which

does not require an assigned probability distribution function can resolve the 180° directional ambiguity inherent in other GNSS-R and radar scatterometry processing methods. Retrieval of roughness characteristics using relatively powerful signals of opportunity from S-band satellite radio broadcasts produced SNR values greatly exceeding those of GPS transmissions [56]. These broadcasts can provide high-quality GNSS-R + data along the coastal margins but are not available over the deep ocean.

Useful reviews of ground-based and airborne GNSS-R campaigns, geophysical models and signal processing techniques for a variety of oceanographic applications are available [2,44]. Campaigns performed over ocean surfaces have spanned locations in the North Sea, the Baltic Sea, the Mediterranean Sea and the Atlantic Ocean [44], and the Tasman Sea in the western South Pacific [39]. Newly developed GNSS-R signal processing techniques, exploiting favourable sampling geometries or instrument refinements, can now be used to extract such factors as significant wave height and roughness field directionality [38,54] or to relate ocean roughness to surface brightness temperature measured at microwave frequencies [57,58]. The possibility of retrieving ocean surface temperature and salinity from permittivity estimates derived from polarimetric GNSS-R measurements has also been investigated [59]. Such a development could complement the retrieval of sea surface salinity from current L-band radiometry missions (ESA's SMOS and NASA's Aquarius), which is strongly affected by the influence of roughness effects on emissivity.

A well-established approach to estimate sea state and wind speed using GNSS-R measurements is based on the theoretical model of [60], which solves the bistatic radar equation of the time-delayed scattered power for the radar cross section σ_0:

$$\left\langle |Y(\tau,f_c)|^2 \right\rangle = T_i^2 \iint_A \frac{G^2(\vec{\rho})|S(f_c - f_D(\vec{\rho}))|^2 \Lambda^2 \left(\tau - (R_0(\vec{\rho}) - R(\vec{\rho}))/c\right)}{4\pi R_0^2(\vec{\rho}) R^2(\vec{\rho})} \sigma_0(\vec{\rho})\, d^2\vec{\rho} \quad (2)$$

Here, τ is the time delay relative to the specular reflection; T_i is the averaging time; A is the reflecting surface area; $\vec{\rho}$ is the reflecting surface position vector; and R_0 and R are the distances from a surface point to the transmitter and receiver, respectively; and f_c and f_D are the frequencies of the replica signal and the reflected Doppler signal, respectively. The terms G, S and Λ represent the antenna pattern, the sinc function for the Doppler mismatch and the navigation signal correlation function, respectively. In general, this equation is solved in 2D delay Doppler space using various geometric descriptions of the corresponding DDM [61]. However, it is often simpler and faster to perform retrievals in 1D delay space by deriving the corresponding delay waveforms. In the limit set by the geometric optics theory, σ_0 is proportional to the probability density function of surface gravity wave slopes from which the mean square slope (MSS) may be derived. A semi-empirical wind-wave spectrum [62] is typically used to infer wind speed at standard meteorological height from the derived MSS.

An example of wind speed estimation, based on the model fitting method, appears in Figure 4 [63]. Five theoretical 1D delay waveforms are shown corresponding to five different wind speeds (3, 4, 5, 6 and 7 m/s), with a measured delay waveform from GPS satellite PRN#13 superimposed. The data were collected by an airborne receiver at an altitude of about 3 km. The measured waveform is the result of coherent integration of 1-ms intermediate frequency (IF) signals followed by incoherent integration of 1,000 of these 1-ms integrals. The measured waveform matches well with the theoretical waveform of wind speed 4 m/s, which closely matches the observed wind speed of 4.4 m/s.

Recent successes in global mapping of sea surface salinity using L-band radiometers aboard ESA's SMOS and NASA's Aquarius satellites provide additional motivation for developing techniques to deduce corrections for roughness influence on L-band emissivity. Several airborne missions have demonstrated this potential, and the planned launch of NASA's Cyclone Global Navigation Satellite System (CYGNSS) L-band reflectometer constellation in 2016, with the goal of mapping surface winds at a high temporal resolution inside tropical cyclones, will allow this concept to be tested in space. Recent extensions of GNSS-R to communications satellites operating on higher frequency bands, with improved signal strength, demonstrate enhanced precision of ocean reflectometry measurements

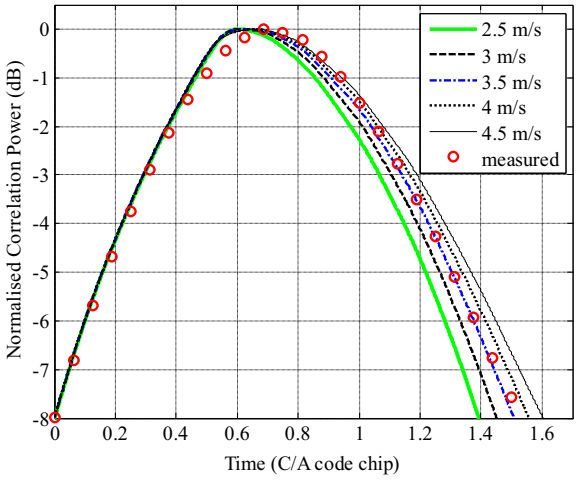

Figure 4 Wind speed estimation through matching the measured delay waveform with modelled waveforms.

with the possibility of expanded coverage in coastal regions [43,56,64].

Land applications

Knowledge of soil moisture content is critical for drought and irrigation management, so as to increase crop yields and to gain a better understanding of natural processes linked to the water, energy and carbon cycles. Soil moisture can be estimated by analysing surface-scattered signals transmitted and received by active radar sensors or natural surface emission detected by microwave radiometers. Alternatively, GNSS-R signals can be employed to estimate soil moisture. Since the soil dielectric constant and reflectivity depend on soil moisture, the variation in the reflected GNSS signal power, or SNR, indicates changes in soil moisture [65]. If feasible, the empirical dielectric model based method in [66] may be applied to GNSS-based soil moisture retrieval. In this method, the transition moisture parameter (θ_t) is defined as

$$\theta_t = 0.165 + 0.49\theta_{wt} \quad (3)$$

where θ_{wt} is the wilting point moisture that is a function of the percentage of the clay and sand contents. Depending on whether the soil moisture is greater or less than the transition moisture, a specific formula can be used to calculate the soil moisture. This model employs the mixing of either the dielectric constants or the refraction indices of ice, water, rock and air and treats the transition moisture value as an adjustable parameter. The dielectric constant of the soil can be estimated by measuring the surface reflectivity. The model is quite general since it was developed by considering many different types of soils.

An alternative GNSS-R technique for soil moisture estimation is the interferometric method in which the power associated with the coherent sum of the direct and reflected GNSS signals is exploited. After continuously measuring the total power for a few hours, the location of the power notch over satellite elevation can be observed, and the soil moisture may be estimated [67]. This notch-based approach is limited to the case where a vertically polarised antenna is used and fixed as horizon-looking. It would not be applicable to standard geodetic antennas. It is an advantage to use existing GPS receivers, installed primarily for geophysical and geodetic applications, to estimate soil moisture [66]. The zenith-looking antenna at a geodetic reference receiver station captures both direct and reflected GPS signals, although the reflected signals are received at a negative elevation angle where the antenna radiation gain is non-zero. The amplitude (or SNR) and phase (or frequency) of the multipath signal can be used to infer soil moisture information [68]. These receivers, if exploited effectively, could provide a global network for services on soil moisture, vegetation and snow cover [69,70]. GNSS-based soil moisture estimation is complicated by a number of issues including surface roughness, vegetation canopy and variation in percentage of individual soil components. To achieve reliable soil moisture estimation, these issues must be taken into account through processes such as modelling and compensation.

Forest change detection is another possible application of GNSS remote sensing. Forest change can provide useful information about global climate change impacts and carbon storage, and knowledge of forest change is vital for effective forest management. Received signal strength of the reflected GNSS signals can be employed to distinguish forest conditions from each other, since different surface covers have different reflectivities. A number of signal strength ranges may be defined to be associated with a group of surfaces such as lake/river water, typical dense forest and cleared area due to logging [71]. Figure 5 shows four ground specular reflection tracks of the reflected signals from four GNSS satellites received by a receiver on an aircraft. The tracks are colourised by the reflected signal power. The low signal power corresponds to the dense forest areas, while the high signal power occurs over three areas marked by A1 (cleared area), A2 (partially cleared area) and A3 (lake water). Accordingly, a surface can be classified by determining within which range its measured strength falls. In addition to signal strength, other signal characteristics such as those related to the observed correlation waveform may be used to enhance surface change detection or surface classification. The major issue related to surface change detection is the dependence of reflectivity on several factors such as soil moisture and surface roughness. Forest change may be quantified by evaluating forest biomass, which depends on the volume of both living and dead trees (leaves, branches and trunks). The received signal power can be used to determine the scattering coefficient which, based on simulation [72], should be a function of the biomass. However, it is a challenging problem to derive a formula that accurately describes the relationship between the scattering coefficient and the biomass.

Cryosphere applications

GNSS-R has been used to sense sea ice and snow, mid- to high-latitude continental snow and deep sub-surface layers of Antarctica's dry snow. Three main parameters of sea ice (i.e. thickness, surface roughness and ice permittivity) can be retrieved with GNSS-R. These parameters can be combined to help characterise different ice types including new ice, young ice, thin first-year ice, first-year ice, and multiyear ice. Sea ice thickness is a key parameter for classification and characterisation of sea ice masses, which influence the temperature and circulation pattern of both the ocean and atmosphere and thus

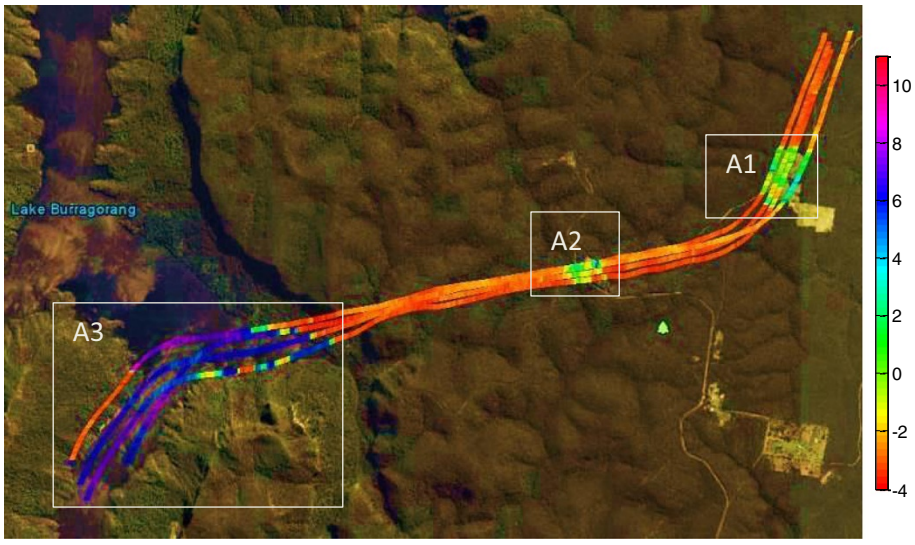

Figure 5 Ground specular reflection tracks associated with four GPS satellites, colourised by reflected signal power. The picture was generated by Google Earth and GPS Visualizer.

can be used for analyses of the Earth's climate. In the case of reflections over a sea ice surface, it is possible to track phase delay precisely so as to retrieve the ice thickness through phase altimetry. ESA initiated a GPS sea-ice campaign, and a ground-based experiment was conducted in Greenland over a 7-month period in order that the complete process of sea ice formation and melting was monitored [73,74]. The time series of the retrieved heights is in agreement with an Arctic tide model, and there is a consistency between results obtained using different antenna polarisations.

Similar to sea surface wind speed retrieval, model fitting between the theoretical and measured delay waveforms can be used to determine the roughness of an ice surface [75]. In the transition from newly formed sea ice to older and thicker ice, a gradual decrease was observed in bulk salinity and an increase in surface roughness. Roughness may also be inferred by investigating the characteristics of the phase or coherence of the interferometric signal [73,76]. Permittivity of sea ice is another important parameter which can be estimated by determining the ratio between the co-polar and cross-polar components of the reflected signal [44,76] or by model fitting of delay waveform [77].

Snow is a critical storage component in the hydrologic cycle and an important component of the climate system; however, current in situ observations of snow distribution are sparse. By making use of the networks of GPS stations established for geodetic applications, it is possible to monitor snow distribution on a global scale. The SNR and phase of the multipath signal are both a function of the antenna height above the ground. The presence of a snow pack around the antenna reduces the antenna height and hence changes the multipath signal SNR [78,79]. The multipath signal SNR is a periodic function with a carrier phase given by

$$\varphi_m = \frac{4\pi h}{\lambda} \sin\theta \tag{4}$$

where h is the antenna height relative to the ground surface, λ is the wavelength, and θ is the satellite elevation angle. Differentiating the phase with respect to sin θ will produce the signal frequency

$$f_m = \frac{2h}{\lambda} \tag{5}$$

As a consequence, the antenna height, and hence the snow depth, can be estimated by measuring the frequency of the multipath signal SNR. It is worth mentioning that GNSS signal reflection off Antarctic dry snow can be significantly different from that of typical wet snow surfaces. The L-band GNSS signals can penetrate into the dry snow down to 200 to 300 m, producing a complex interference pattern induced by the multiple reflections occurring at different layer interfaces of the sheet [80]. Radio-holographic techniques are used on each lag of the delay waveform to identify the spectral content of the signal and to identify each frequency component to different snow depths.

Missions

Useful reviews of radio occultation missions can be found in [81] and [82]. The concept was first proved by the GPS/MET (GPS/Meteorology) satellite mission in 1995 to 1997. That satellite took few measurements but was followed

by the more productive CHAllenging Minisatellite Payload (CHAMP) and Satellite de Aplicaciones Cientificas-C (SAC-C) satellites. CHAMP provided 8 years of radio occultation data consisting of around 440,000 measurements from February 2001 to October 2008 [83]. Those missions led to the launch in 2006 of a six-satellite constellation FORMOSAT-3/COSMIC, which provided 1,500 to 2,000 soundings per day, resulting in GPS RO becoming an operational data source for weather prediction and ionospheric monitoring. Other missions that provided significant quantities of RO data are Gravity Recovery and Climate Experiment (GRACE-A), METeorological Operations (METOP-A), Communications/Navigation Outage Forecasting System (C/NOFS), TerraSAR-X and TanDEM-X. Table 1 (taken from the COSMIC website [84]) shows the contributions made by these and other missions to both atmospheric and ionospheric sounding. With the COSMIC constellation degrading, as it has reached its design life, a new FORMOSAT-7/COSMIC-2 follow-on constellation is being constructed which has multifrequency, multi-GNSS receivers onboard 12 satellites to be launched - six into low-inclination orbits in 2015 and six into high-inclination orbits in 2018 [85].

Far fewer satellites have been able to perform GNSS reflectometry. The first was UK-DMC from 2003 to 2011 [86]. Others that have been proposed are Techdemosat-1 launched July 2014 [87] with a custom reflectometry payload; PARIS, a dedicated mission for GNSS-R [35,88]; CYGNSS, a constellation of eight microsatellites [89]; GEROS-ISS (GNSS REflectometry, Radio Occultation and Scatterometry onboard International Space Station) [90]; and Cat-2 [91]. Several of the authors are also from the University of New South Wales (UNSW), which is preparing a CubeSat to carry both GNSS occultation and reflectometry experiments as part of the QB50 mission [92]. As illustrated in Figure 1, a LEO satellite to be launched for the QB50 mission can receive the direct, reflected and refracted GNSS signals to enable positioning, reflectometry and occultation applications.

Table 1 Contributions to atmospheric and ionospheric sounding by missions

MISSION	Total atm occs	Total ion occs
CHAMP	399,968	303,291
CNOFS	120,588	0
COSMIC	4,039,311	3,707,966
GPSMET	5,002	0
GPSMETSA	4,666	0
GRACE	273,013	132,817
METOPA	993,084	0
SACC	353,808	0
TSX	276,549	0
Total	6,465,989	4,144,074

Data obtained from the COSMIC website [84] (last updated: Sat Dec 7 23:25:02 MST 2013).

Instruments

Even though primarily designed for precise navigation, surveying and geodesy, high-end dual-frequency GPS receivers have been used for more than two decades for a diverse set of remote sensing applications. Ground-based receiver networks such as that maintained by the International GNSS Service (IGS) are routinely used to monitor the tropospheric vapour content and the ionospheric electron content. Multifrequency, multiconstellation receivers that are now available will further improve the spatial and temporal resolution in the near future. With slight modifications of standard geodetic receivers (higher data rate, special observation types), the so-called scintillation receivers can be used to study the short-term variability of the atmosphere, including scintillation, ionospheric storms or travelling ionospheric disturbances [93].

For satellite-borne GNSS applications, various modifications of terrestrial receivers are required, including hardware and software modifications to enhance survivability in a space environment (temperature, vacuum, radiation) and to ensure a proper acquisition of signals despite the high orbital velocity and the associated Doppler shifts. On the other hand, special hardware and software is required to support non-navigation remote sensing applications in space, such as radio occultation measurements. Well-known examples include the BlackJack and Integrated GPS Occultation Receiver (IGOR) flown on numerous research satellites [94], or the GRAS instrument flown on MetOp as shown in Figure 6 [95]. These offer a high-rate sampling (50 Hz to 1 KHz) of raw phase observations or correlator outputs and open-loop tracking techniques. A model of the expected Doppler shift is used during occultations in the deep layers of the atmosphere to facilitate tracking at very low signal levels. Radio occultation receivers are also operated with special beam-forming antennas to increase the antenna gain in directions close to the Earth's limb [95].

While the applications discussed so far can largely be fulfilled with receivers using traditional correlator application-specific integrated circuits (ASICs), GNSS-R calls for a higher flexibility in the receiver design. As discussed in the previous sections, GNSS-R may be used for a variety of remote sensing applications such as studies of the sea surface height and roughness or salinity and soil moisture from the properties of passively reflected GNSS signals. Besides special antennas (down-looking, high-gain or beam-steering antennas with left-hand polarisation) [35], such receivers commonly employ a large number of slaved correlators and often exceed the capabilities of traditional ASICs. This is even truer for new advanced signal processing techniques. Recently, two novel correlation schemes

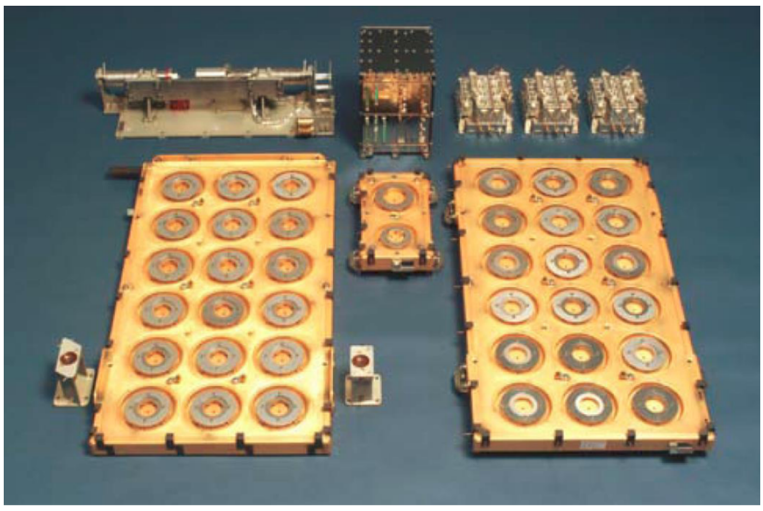

Figure 6 Image of the GRAS instrument flown on MetOp-A. Images showing the GRAS instrument with both occultation antennas (front left and front right), the Zenith antenna (front middle) and the R/F front ends and main electronics unit (in the back).

have been introduced: the so-called interferometric processing [35] and the direct-signal-enhanced semi-codeless processing [96]. Both methods do not correlate the reflected signal with a clean replica signal, but directly cross-correlate the line-of-sight signal received from a zenith-looking antenna either with the reflected signal from a nadir-looking antenna for the first method or with a modelled replica of the encrypted signal obtained in a semi-codeless way for the second method. Key advantages of these new schemes are that no prior knowledge of the incoming signal is required and there is a significant improvement in the measurement precision and the carrier to noise ratio. For altimetric applications in particular, which are probably the most demanding applications in terms of the required instrument hardware and processing capabilities, this is of crucial benefit.

The disadvantage of these novel methods is that the correlation requires a substantially increased signal processing effort. To cope with these needs, a software-defined radio approach is widely applied. In the extreme case, pure software receivers have been employed by various research groups for offline processing of the pre-recorded radio frequency (RF) signals, while field-programmable gate arrays (FPGA) or fast digital signal processors (DSPs) are commonly used in real-time-capable reflectometry receivers. Examples of the latter type of receivers include the GOLD-RTR [97] and SSTL's SGR-ReSI [98] instruments developed by IEEC, Barcelona, and SSTL, Surrey, respectively.

Challenging issues and future directions

GNSS has a global space-based positioning, navigation and timing (PNT) capability. There are many technological challenges for GNSS remote sensing to come close to matching the extraordinary success of GNSS-PNT, especially in the case of the GNSS-R technique. Satellite-borne GNSS remote sensing must demonstrate its value as a reliable, continuous, high-quality sensing technology. With the launch of multiple LEO satellites with GNSS-RO- and GNSS-R-capable instrumentation, it seems we are at last close to a renaissance. But are more LEO missions and better algorithms for geophysical parameter extraction sufficient? In the case of GNSS-RO, the answer is yes because the meteorological/climate community now assimilates GNSS-RO products into their operational and research systems and is eager for more [11-15]. However, GNSS-R is still very much a novelty technology as far as the geosciences community is concerned because current results are generated by one or more isolated academic group and not organised into independently verifiable products. Nevertheless, as mentioned earlier, it is a fact that the Plate Boundary network is being used in the USA for a range of GNSS-R applications.

The International Association of Geodesy (IAG) has been very successful in launching technique-specific services (see [99]). These services aid other geoscientists in their research, as well as supporting important applications in the wider community. Examples of the latter are the contribution of the International GNSS Service (IGS) to precise positioning [100] and the International Earth Rotation and Reference Systems Service (IERS) to the International Terrestrial Reference Frame (ITRF) [101]. The IGS does generate troposphere and ionosphere parameter products [102]; however, they are based on observations made from the global ground-based GNSS tracking network (Figure 7), not from satellite platforms. There are no geodetic services producing GNSS remote sensing products on a continuous, synoptic basis. From the IAG's perspective, the challenging issues

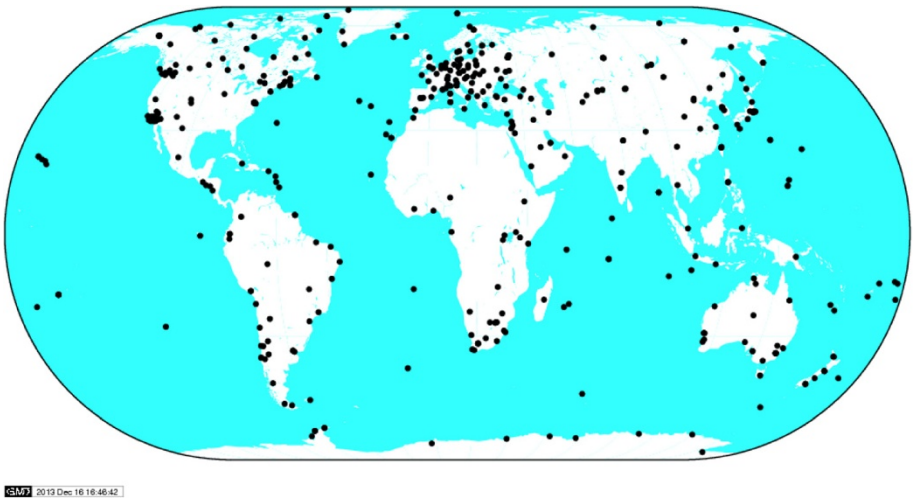

Figure 7 IGS observations made from the global ground-based GNSS tracking network. One of the reasons for the success of IAG services are the permanent geodetic observing networks such as IGS's global GNSS tracking network, providing accurate, reliable data products for science and society.

are related to 'operationalising' GNSS remote sensing, in all its forms, so that the remotely sensed geophysical parameters (atmospheric, oceanic, wind, soil moisture, biomass, etc.) are included in the suite of geodetic outputs of the Global Geodetic Observing System (GGOS) [103].

The non-technical challenges therefore include the evolution of current GNSS remote sensing science missions to operational services by *increasing* the number of LEO satellites equipped with GNSS receivers to satisfy coverage requirements in space and time; *standardising* data formats, instrumentation, and calibration, pre-processing and analysis procedures; and establishing a *coordinating* agency or authority so as to ensure continuous, high-quality product generation and dissemination. The IAG has considerable experience with geometry technique-based services (such as the IGS, ILRS, IVS and IDS) [104]; however, it has not yet established any 'geodetic imaging' services based on technologies such as synthetic aperture radar (SAR), satellite radar altimetry, lidar or GNSS remote sensing (GNSS-RO, GNSS-R). One of the future challenges is to address this shortcoming, so that GNSS remote sensing can be recognised as a geodetic technique that is making critical contributions to science and society.

Conclusions

This paper provided an overview of GNSS remote sensing (GNSS-RO and GNSS-R) with a focus on six different issues. Atmospheric sensing using GNSS-RO measurements has been extensively investigated for determining atmospheric parameters such as water vapour, temperature, pressure and humidity. Significant benefits have been shown for the southern hemisphere where there is limited access to ground-based observations, and GNSS-RO has been operationally used by major international weather forecasting models. GNSS-R, on the other hand, which has recently gained more attention from research organisations and universities, can be used to perform remote sensing tasks related to ocean observation and land applications, retrieving a wide range of geophysical parameters including sea surface wind speed and direction, sea surface height and roughness, soil moisture, biomass, snow/ice depth, coverage and density. The most important past and planned satellite missions primarily associated with GNSS-RO and GNSS-R applications were summarised. More GNSS-RO missions have been launched, while a few GNSS-R missions are planned. The state-of-the-art characteristics of the GNSS receiver were discussed, which is the key equipment for GNSS remote sensing. Finally, a number of challenging issues related to GNSS remote sensing products and services were highlighted.

Competing interests

The authors declare that they have no competing interests.

Author details

[1]School of Geodesy and Geomatics, Wuhan University, Wuhan 430079, China. [2]School of Civil and Environmental Engineering, UNSW, Sydney, NSW 2052, Australia. [3]Oceanography Division, Naval Research Laboratory, Stennis Space Center, MS 39529, USA. [4]Australian Centre for Space Engineering Research, School of Electrical Engineering and Telecommunications, UNSW, Sydney, NSW 2052, Australia. [5]SPACE Research Centre, RMIT University, Melbourne, VIC 3001, Australia. [6]Section Space Flight Technology, German Space Operations Center (DLR), 82234 Wessling, Germany.

Received: 2 April 2014 Accepted: 15 August 2014
Published: 27 August 2014

References

1. S Gleason, D Gebre-Egziabher, *GNSS Applications and Methods* (Artech House, Boston, 2009)

2. S Jin, E Cardellach, F Xie, *GNSS Remote Sensing: Theory, Methods and Applications* (Springer, Dordrecht, 2014)
3. Y-A Liou, AG Pavelyev, S-F Liu, AA Pavelyev, N Yen, C-Y Huang, G-J Fong, FORMOSAT-3/COSMIC GPS radio occultation mission: preliminary results. IEEE Trans Geosci Rem Sens **45**(11), 3813–3826 (2007)
4. AG Pavelyev, K Zhang, Y-A Liou, AA Pavelyev, C-S Wang, J Wickert, T Schmidt, Y Kuleshov, Principle of locality and analysis of radio occultation data. IEEE Trans Geosci Rem Sens **51**(6), 3240–3249 (2013)
5. AG Pavelyev, K Zhang, SS Matyugov, YY-A Liou, C-S Wang, OI Yakovlev, IA Kucherjavenkov, Y Kuleshov, Analytical model of bistatic reflections and radio occultation signals. Radio Sci **46**(RS1009), (2011). doi:10.1029/2010RS004434
6. A Rius, G Ruffini, A Romeo, Analysis of ionospheric electron density distribution from GPS/MET occultations. IEEE Trans Geosci Rem Sens **36**(2), 383–394 (1998)
7. YT Yoon, M Eineder, N Yague-Martinez, O Montenbruck, TerraSAR-X precise trajectory estimation and quality assessment. IEEE Trans Geosci Rem Sens **47**(5), 1859–1868 (2009)
8. RJ Norman, PL Dyson, E Yizengaw, JL Marshall, C-S Wang, BA Carter, D Wen, K Zhang, Radio occultation measurements from the Australian microsatellite FedSat. IEEE Trans Geosci Rem Sens **50**(11), 4832–4839 (2012)
9. H Li, Y Yuan, Z Li, X Huo, W Yan, Ionospheric electron concentration imaging using combination of LEO satellite data with ground-based GPS observations over China. IEEE Trans Geosci Rem Sens **50**(3), 1728–1735 (2012)
10. K Zhang, E Fu, D Silcock, Y Wang, Y Kuleshov, An investigation of atmospheric temperature profiles in the Australian region using collocated GPS radio occultation and radiosonde data. Atmos Meas Tech **4**, 2087–2092 (2011)
11. J Le Marshall, Y Xiao, R Norman, K Zhang, A Rea, L Cucurull, R Seecamp, P Steinle, K Puri, E Fu, T Le, The application of radio occultation observations for climate monitoring and numerical weather prediction in the Australian Region. Aust Meteorol Oceanogr J **62**, 323–334 (2012)
12. C Cardinali, Forecast sensitivity to observation (FSO) as a diagnostic tool. ECMWF Tech Memo **599**, (2009)
13. SB Healy, AM Jupp, C Marquardt, Forecast impact experiment with GPS radio occultation measurements. Geophys Res Lett. (2005). doi:10.1029/2004GL020806
14. L Cucurull, JC Derber, Operational implementation of COSMIC observations into NCEP's global data assimilation system. Weather Forecast **23**, 702–711 (2008)
15. RA Anthes, PA Bernhardt, Y Chen, L Cucurull, KF Dymond, D Ector, SB Healy, S-P Ho, DC Hunt, Y-H Kuo, H Liu, K Manning, C McCormick, TK Meehan, WJ Randel, C Rocken, WS Schreiner, SV Sokolovskiy, S Syndergaard, DC Thompson, KE Trenberth, T-K Wee, NL Yen, Z Zeng, The COSMIC/FORMOSAT-3 Mission: early results. Bull Am Meteorol Soc **89**, 313–333 (2008)
16. R Norman, J LeMarshall, W Rohm, B Carter, C Liu, K Zhang, The impact of severe weather events on GPS signal propagation. IEEE Int J Appl Earth Obs Rem Sens **7**(8), (2014). in press
17. Y Li, G Kirchengast, B Scherllin-Pirscher, S Wu, M Schwaerz, J Fritzer, S Zhang, B Carter, K Zhang, A new dynamic approach for statistical optimization of GNSS radio occultation bending angles for optimal climate monitoring utility. J Geophys Res **118**(23), 13,022–13,040 (2014)
18. CS Wang, R Norman, TK Yeh, K Zhang, SL Choy, TP Tseng, Investigation into the atmospheric parameters retrieved from ROPP and CDAAC using GPS radio occultation measurements over the Australian area. Aust J Earth Sci (2014). doi:10.1080/08120099.2014.924555
19. CL Liu, G Kirchengast, K Zhang, R Norman, Y Li, SC Zhang, B Carter, J Fritzer, M Schwaerz, SL Choy, SQ Wu, ZX Tan, Characterisation of residual ionospheric errors in bending angles using GNSS RO end-to-end simulations. Adv Space Res **52**, 821–836 (2013)
20. AK Steiner, D Hunt, S-P Ho, G Kirchengast, AJ Mannucci, B Scherllin-Pirscher, H Gleisner, A von Engeln, T Schmidt, C Ao, SS Leroy, ER Kursinski, U Foelsche, M Gorbunov, S Heise, Y-H Kuo, KB Lauritsen, C Marquardt, C Rocken, W Schreiner, S Sokolovskiy, S Syndergaard, J Wickert, Quantification of structural uncertainty in climate data records from GPS radio occultation. Atmos Chem Phys **13**, 1469–1484 (2013)
21. E Cardellach, S Tomas, S Oliveras, R Padullés, A Rius, M De, FJ la Torre-Juárez, COA Turk, ER Kursinski, B Schreiner, D Ector, L Cucurull, Sensitivity of PAZ LEO polarimetric GNSS radio-occultation experiment to precipitation events. IEEE Trans Geosci Rem Sens **53**(1), 190–2016 (2015)
22. A Flores, G Ruffini, A Rius, 4D tropospheric tomography using GPS slant wet delays. Ann Geophys **18**, 223–234 (2000)
23. H Seko, S Shimada, H Nakamura, T Kato, Three-dimensional distribution of water vapor estimated from tropospheric delay of GPS data in a mesoscale precipitation system of the Baiu front. Earth Planets Space **52**, 927–933 (2000)
24. T Nilsson, L Gradinarsky, Water vapor tomography using GPS phase observations: simulation results. IEEE Trans Geosci Rem Sens **44**(10), 2927–2941 (2006)
25. M Bender, A Raabe, Preconditions to ground-based GPS water vapour tomography. Ann Geophys **25**(8), 1727–1734 (2007)
26. W Rohm, K Zhang, J Bosy, Limited constraint, robust Kalman filtering for GNSS troposphere tomography. Atmos Meas Tech **7**, 1475–1486 (2014)
27. W Rohm, Y Yuan, B BiadegIgne, K Zhang, M JLe, Ground-based GNSS ZTD/IWV estimation system for numerical weather prediction in challenging weather conditions. Atmos Res **138**, 414–426 (2014)
28. Y Yuan, K Zhang, W Rohm, S Choy, R Norman, C Wang, Real time retrieval of atmospheric water vapour from GPS precise point positioning. J Geophys Res, (2014). doi:10.1002/2014JD021486
29. S Choy, C Wang, K Zhang, Y Kuleshov, GPS sensing of precipitable water vapour during the March 2010 Melbourne storm. Adv Space Res **52**(9), 1688–1699 (2013)
30. T Manning, *Sensing the dynamics of severe weather using 4D GPS tomography in the Australian region* (PhD thesis, RMIT University, 2014), p. 196
31. T Manning, K Zhang, W Rohm, S Choy, F Hurter, Detecting severe weather in Australia using GPS tomography. J GPS **11**(1), 58–70 (2012)
32. GV Bennitt, A Jupp, Operational assimilation of GPS zenith total delay observations into the Met Office Numerical Weather Prediction Models. Mon Weather Rev **140**(8), 2706–2719 (2012)
33. R Treuhaft, ST Lowe, C Zuffada, Y Chao, 2-cm GPS altimetry over Crater Lake. Geophys Res Lett **28**(23), 4343–4346 (2001)
34. M Martin-Neira, A passive reflectometry and interferometry system (PARIS): application to ocean altimetry. ESA J **17**, 331–335 (1993)
35. M Martin-Neira, S D'Addio, C Buck, N Floury, R Prieto-Cerdeira, The PARIS ocean altimeter in-orbit demonstrator. IEEE Trans Geosci Rem Sens **49**(6), 2209–2237 (2011)
36. M Martin-Neira, S D'Addio, R Vitulli, Study of delay drift in GNSS-R altimetry. IEEE Int J Appl Earth Obs Rem Sens **7**(5), 1473–1480 (2014)
37. D Pascual, A Camps, F Martin, H Park, A Alonso Arroyo, R Onrubia, Precision bounds in GNSS-R ocean altimetry. IEEE Int J Appl Earth Obs Rem Sens **7**(5), 1416–1423 (2014)
38. A Rius, E Cardellach, M Martın-Neira, Altimetric analysis of the sea-surface GPS-reflected signals. IEEE Trans Geosci Rem Sens **48**(4), 2119–2127 (2010)
39. K Yu, C Rizos, A Dempster, GNSS-based model-free sea surface height estimation in unknown sea state scenarios. IEEE Int J Appl Earth Obs Rem Sens **7**(5), 1424–1435 (2014)
40. S Lowe, T Meehan, L Young, Direct-signal enhanced semi-codeless processing of GNSS surface-reflected signals. IEEE Int J Appl Earth Obs Rem Sens **7**(5), 1469–1472 (2014)
41. S D'Addio, M Martin-Neira, M di Bisceglie, C Galdi, F Martin Alemany, GNSS-R altimeter based on Doppler multi-looking. IEEE Int J Appl Earth Obs Rem Sens **7**(5), 1452–1460 (2014)
42. ST Lowe, C Zuffada, Y Chao, P Kroger, LE Young, JL LaBrecque, 5-cm precision aircraft ocean altimetry using GPS reflections. Geophys. Res Lett **29**(10), 1375 (2002). doi:10.1029/2002GL014759
43. S Ribó, JC Arco, S Oliveras, E Cardellach, A Rius, C Buck, Experimental results of an X-Band PARIS receiver using digital satellite TV opportunity signals scattered on the sea surface. IEEE Trans Geosci Rem Sens **52**(2014), (2014). doi:10.1109/TGRS.2013.2292007
44. E Cardellach, F Fabra, O Nogues-Correig, S Oliveras, S Ribo, A Rius, GNSS-R ground-based and airborne campaigns for ocean, land, ice and snow techniques: application to the GOLD-RTR data sets. Radio Sci **46**(6), 1412–1415 (2011). RS0C04, doi:10.1029/2011RS004683
45. JL Garrison, E Cardellach, S Gleason, S Katzberg, Foreword to special issue on reflectometry using global navigation satellite systems and other signals of opportunity (GNSS + R). IEEE Int J Appl Earth Obs Rem Sens **7**(5), 1412–1415 (2014)
46. JL Garrison, SJ Katzberg, MI Hill, Effect of sea roughness on bistatically scattered range coded signals from the Global Positioning System. Geophys Res Lett **25**(13), 2257–2260 (1998)

47. S Gleason, SS Hodgart, Y Sun, C Gommenginger, S Mackin, M Adjrad, M Unwin, Detection and processing of bistatically reflected GPS signals from low earth orbit for the purpose of ocean remote sensing. IEEE Trans Geosci Rem Sens **43**(6), 1229–1241 (2005)
48. E Cardellach, G Ruffini, D Pino, A Rius, A Komjathy, JL Garrison, Mediterranean balloon experiment: ocean wind speed sensing from the stratosphere using GPS reflections. Remote Sens Environ **88**(3), 351–362 (2003)
49. SJ Katzberg, RA Walker, JH Roles, T Lynch, PG Black, First GPS signals reflected from the interior of a tropical storm: preliminary results from Hurricane Michael. Geophys Res Lett **28**(10), 1981–1984 (2001)
50. SJ Katzberg, J Dunion, Comparison of reflected GPS wind speed retrievals with dropsondes in tropical cyclones. Geophys Res Lett **36**(L17602), (2009). doi:10.1029/2009GL039512
51. SJ Katzberg, O Torres, G Ganoe, Calibration of reflected GPS for tropical storm wind speed retrievals. Geophys Res Lett **33**(L18602), (2006). doi:10.1029/2006GL026825
52. N Rodriguez-Alvarez, DM Akos, VU Zavorotny, JA Smith, A Camps, CW Fairall, Airborne GNSS-R wind retrievals using delay-Doppler maps. IEEE Trans Geosci Rem Sens **51**(1), 626–641 (2013)
53. O Germain, G Ruffini, F Soulat, M Caparrini, B Chapron, P Silverstrin, The Eddy Experiment: GNSS-R speculometry for directional sea-roughness retrieval from low altitude aircraft. Geophys Res Lett **31**(L21307), 1–4 (2004)
54. A Komjathy, M Armatys, D Masters, P Axelrad, Retrieval of ocean surface wind speed and wind direction using reflected GPS signals. J Atmos Ocean Technol **21**, 515–526 (2004)
55. E Cardellach, A Rius, A new technique to sense non-Gaussian features of the sea surface from L-band bi-static GNSS reflections. Rem Sens Environ **112**(6), 2927–2937 (2008)
56. R Shah, J Garrison, M Grant, Demonstration of bistatic radar for ocean remote sensing using communication satellite signals. IEEE Geosci Remote Sens Lett **9**(4), 619–623 (2012)
57. JF Marchan-Hernandez, N Rodriguez-Alvarez, A Camps, X Bosch-Lluis, I Ramos-Perez, E Valencia, Correction of the sea state impact in the L-band brightness temperature by means of delay Doppler maps of Global Navigation Satellite signals reflected over the sea surface. IEEE Trans Geosci Rem Sens **46**(10), 29142923 (2008)
58. E Valencia, A Camps, N Rodriguez-Alvarez, I Ramos-Perez, X Boxch-Lluis, H Park, Improving the accuracy of sea surface salinity retrieval using GNSS-R data to correct the sea state effect. Radio Sci **46**(RS0C02), 1–11 (2011)
59. E Cardellach, S Ribó, A Rius, *Technical Note on POlarimetric Phase Interferometry (POPI)* (CSIC-IEEC, 2006). arXiv:physics/0606099 2
60. VU Zavorotny, AG Voronovich, Scattering of GPS signals from the ocean with wind remote sensing application. IEEE Trans Geosci Rem Sens **38**(2), 951–963 (2000)
61. T Elfouhaily, DR Thompson, L Linstrom, Delay-Doppler analysis of bistatically reflected signals from the ocean surface: theory and application. IEEE Trans Geosci Rem Sens **40**(3), 560–573 (2002)
62. T Elfouhaily, B Chapron, K Katsaros, D Vandermark, A unified directional spectrum for long and short wind-driven waves. J Geophys Res **102**(C7), 15781–15796 (1997)
63. K Yu, C Rizos, AG Dempster, Sea surface wind speed estimation based on GNSS signal measurements, in *Proceedings of international geoscience and remote sensing symposium (IGARSS)* (Munich, Germany, 2012), pp. 2587–2590
64. JL Garrison, KM Larson, D Burrage, Advancing reflectometry, workshop on reflectometry using GNSS and other signals of opportunity (GNSS + R). Eos **94**(21), 193 (2012)
65. D Masters, P Axelrad, SJ Katzberg, Initial results of land-reflected GPS bistatic radar measurements in SMEX02. Remote Sens Environ **92**, 507–520 (2004)
66. JR Wang, TJ Schmugge, An empirical model for the complex dielectric permittivity of soils as a function of water content. IEEE Trans Geosci Rem Sens **18**(4), 288–295 (1980)
67. N Rodriguez-Alvarez, X Bosch-Lluis, A Camps, M Vall-Llossera, E Valencia, JF Marchan-Hernandez, I Ramos-Perez, Soil moisture retrieval using GNSS-R techniques: experimental results over a bare soil field. IEEE Trans Geosci Rem Sens **47**(11), 3616–3624 (2009)
68. VU Zavorotny, KM Larson, JJ Braun, EE Small, ED Gutmann, AL Bilich, A physical model for GPS multipath caused by land reflection: toward bare soil moisture retrievals. IEEE Int J Appl Earth Obs Rem Sens **3**(1), 100–110 (2010)
69. Colorado GPS Reflections Research Group. http://xenon.colorado.edu/portal/, viewed 5 Aug 2014
70. KM Larson, EE Small, Using GPS to study the terrestrial water cycle. Eos **94**(52), 505–512 (2013)
71. K Yu, C Rizos, A Dempster, Forest change detection using GNSS signal strength measurements, in *Proceedings of international geoscience and remote sensing symposium (IGARSS)* (Melbourne, Australia, 2013), pp. 1003–1006
72. P Ferrazzoli, L Guerriero, N Pierdicca, R Rahmoune, Forest biomass monitoring with GNSS-R: theoretical simulations. Adv Space Res **47**, 1823–1832 (2011)
73. M Semmling, G Beyerle, R Stosius, G Dick, J Wickert, F Fabra, E Cardellach, S Ribó, A Rius, A Helm, SB Yudanov, S D'Addio, Detection of arctic ocean tides using interferometric GNSS-R signals. Geophys. Res Lett **38**(4), (2011). doi:10.1029/2010GL046005
74. F Fabra, E Cardellach, A Rius, S Ribó, S Oliveras, O Nogués-Correig, MB Rivas, M Semmling, S D'Addio, Phase altimetry with dual polarization GNSS-R over sea ice. IEEE Trans Geosci Rem Sens **50**(6), 2112–2121 (2012)
75. M Belmonte, *Bistatic scattering of global positioning system signals from Arctic sea ice* (Ph.D. thesis, University of Colorado at Boulder, Boulder, CO, USA, 2007)
76. F Fabra, *GNSS-R as a Source of Opportunity for Remote Sensing of the Cryosphere* (PhD Dissertation, UPC, Barcelona, 2013)
77. M Belmonte, JA Maslanik, P Axelrad, Bistatic scattering of GPS signals off Arctic sea ice. IEEE Trans Geosci Rem Sens **48**(3), 1548–1553 (2009)
78. KM Larson, E Gutmann, V Zavorotny, J Braun, M Williams, FG Nievinski, Can we measure snow depth with GPS receivers? Geophys. Res Lett **36**(L17502), (2009). doi:10.1029/2009GL039430
79. KM Larson, FG Nievinski, GPS snow sensing: results from the EarthScope Plate Boundary Observatory. GPS Solutions **17**(1), 41–52 (2012)
80. E Cardellach, F Fabra, A Rius, S Pettinato, S DAddio, Characterization of dry-snow sub-structure using GNSS reflected signals. Remote Sens Environ **124**, 122–134 (2012)
81. RA Anthes, Exploring Earth's atmosphere with radio occultation: contributions to weather, climate and space weather. Atmos Meas Tech **4**, 1077–1103 (2011). doi:10.5194/amt-4-1077-2011
82. S Jin, GP Feng, S Gleason, Remote sensing using GNSS signals: current status and future directions. Adv Space Res **47**(10), 1645–1653 (2011)
83. S Heise, J Wickert, C Arras, G Beyerle, A Faber, G Michalak, T Schmidt, F Zus, Reprocessing and application of GPS radio occultation data from CHAMP and GRACE, in *Observation of the System Earth from Space - CHAMP, GRACE, GOCE and Future Mission*, ed. by F By Frank, S Nico, S Wolf-Dieter (Springer, Heidelberg, 2014). GEOTECHNOLOGIEN Science Report No. 20
84. COSMIC. http://www.cosmic.ucar.edu/, viewed 9 Dec 2013
85. FORMOSAT-7/COSMIC-2 (COSMIC-2) Science Mission. http://www.cosmic.ucar.edu/cosmic2/, viewed 9 Dec 2013
86. MJ Unwin, S Gleason, M Brennan, The space GPS reflectometry experiment on the UK disaster monitoring constellation satellite, in *Proceedings of ION-GPS/GNSS* (Portland, OR, 2003)
87. Missions. http://www.sstl.co.uk/Missions/TechDemoSat-1, viewed 9 Dec 2013
88. M Martin-Neira, S D'Addio, C Buck, N Floury, R Prieto-Cerdeira, The PARIS in-orbit demonstrator. Proceedings of IEEE IGARSS **2**, II–322–II–325 (2009)
89. CYGNSS. http://aoss-research.engin.umich.edu/missions/cygnss/, viewed 9 Dec 2013
90. GEROS, GNSS REflectometry, Radio Occultation and Scatterometry onboard International Space Station (GEROS-ISS). http://www.ice.csic.es/en/view_project.php?PID=155, viewed 9 Dec 2013
91. H Carreno-Luengo, A Camps, I Perez-Ramos, G Forte, R Onrubia, R Diez, 3Cat-2: a P(Y) and C/A GNSS-R experimental nano-satellite mission, in *Proceedings of international geoscience and remote sensing symposium (IGARSS)* (Melbourne, Australia, 2013), pp. 843–846
92. ACSER QB50 project. http://www.acser.unsw.edu.au/QB50/index.html, viewed 9 Dec 2013
93. VV Sreeja, M Aquino, B Forte, Z Elmas, C Hancock, GD Franceschi, L Alfonsi, L Spogli, V Romano, B Bougard, JFG Monico, AW Wernik, J-M Sleewaegen, A Canto, EFD Silva, Tackling ionospheric scintillation threat to GNSS in Latin America. J Space Weather Space Clim **1**(1), 1–9 (2011). A05
94. J Wickert, G Michalak, T Schmidt, G Beyerle, C-Z Cheng, SB Healy, S Heise, C-Y Huang, N Jakowski, W Kohler, C Mayer, D Offiler, E Ozawa, AG Pavelyev, M Rothacher, B Tapley, C Arras, GPS radio occultation: results from CHAMP, GRACE and FORMOSAT-3/COSMIC. Terrestrial Atmos Oceanic Sci **20**(1), 35–50 (2009)
95. M Bonnedal, J Christensen, A Carlstrom, A Berg, Metop-GRAS in-orbit instrument performance. GPS Solutions **14**(1), 109–120 (2010)

96. S Lowe, T Meehan, L Young, Direct-signal enhanced semi-codeless processing of GNSS surface-reflected signals. IEEE Int J Appl Earth Obs Rem Sens **7**(5), 1269–1472 (2014)
97. O Nogués-Correig, EC Gali, JS Campderrós, A Rius, A GPS-reflections receiver that computes Doppler/delay maps in real time. IEEE Trans Geosci Rem Sens **45**(1), 156–174 (2007)
98. RV Steenwijk, M Unwin, P Jales, Introducing the SGR-ReSI: A next generation spaceborne GNSS receiver for navigation and remote-sensing, in *Proceedings of ESA workshop on satellite navigation technologies and European workshop on GNSS signals and signal processing (NAVITEC)* (Noordwijk, Netherlands, 2010)
99. International Association of Geodesy (IAG). http://www.iag-aig.org, viewed 11 Dec 2013
100. International GNSS Service (IGS). http://igs.org, viewed 11 Dec 2013
101. International Terrestrial Reference Frame (ITRF). http://itrf.ensg.ign.fr, viewed 11 Dec 2013
102. IGS troposphere and ionosphere parameter products. http://www.igs.org/products, viewed 11 Dec 2013
103. Global Geodetic Observing System (GGOS). http://www.ggos.org, viewed 11 Dec 2013
104. IAG services. http://www.iers.org/nn_10880/IERS/EN/Organization/TechniqueCentres/TC.html?__nnn=true, viewed 11 Dec 2013

doi:10.1186/1687-6180-2014-134
Cite this article as: Yu *et al.*: An overview of GNSS remote sensing. *EURASIP Journal on Advances in Signal Processing* 2014 **2014**:134.